

**Atom-modulated dynamic optical hysteresis in driven-dissipative systems**Jianning Li<sup>1</sup>,<sup>✉</sup> H. Z. Shen,<sup>1</sup> Wei Wang,<sup>1,2</sup> and Xuexi Yi<sup>1,2,\*</sup><sup>1</sup>Center for Quantum Sciences, School of Physics, Northeast Normal University, Changchun 130024, China<sup>2</sup>Center for Advanced Optoelectronic Functional Materials Research, Key Laboratory for UV Light-Emitting Materials and Technology of Ministry of Education, Northeast Normal University, Changchun 130024, China

(Received 11 March 2021; accepted 14 June 2021; published 12 July 2021)

We introduce a two-level atom into a cavity as an ancilla to control the hysteresis of the system where the cavity is described by a driven-dissipative nonlinear Kerr model. We find that the dynamic optical hysteresis can be modulated by changing the atom-cavity coupling strength, and the nonlinearity induced by atom-cavity coupling weakens the Kerr nonlinearity in the weak coupling regime. This leads to the change in the critical point corresponding to the decrease in the hysteresis area. The physics behind the modulation is closely related to the effect of the atom-cavity coupling on the discontinuity of the first nonzero Liouvillian eigenvalue. A relative deviation of the metastable state and target steady state is defined to characterize the relation between the hysteresis and adiabaticity of the system. Taking only two Liouvillian eigenvectors into account in the composite system, we derive an expression for the dependence of the hysteresis area on the sweeping speed and discuss its feature in the slow sweeping limit.

DOI: [10.1103/PhysRevA.104.013709](https://doi.org/10.1103/PhysRevA.104.013709)**I. INTRODUCTION**

The classical phase transitions are driven by a competition between the energy of a system and the entropy of its thermal fluctuations. They cannot occur at the zero-temperature limit as the system has no entropy. The phase order is determined by the first discontinuous derivative of thermodynamic potential, and the transition can be understood as the spontaneous symmetry breaking characterized by the change in order parameters [1]. In quantum systems, however, the quantum phase transitions (QPTs) that occur at zero temperature are caused by quantum fluctuations and described as an abrupt change (discontinuity) in the ground state energy of a many-body system at the critical point [2]. There are many intriguing features connected with QPT [3–5], for example, the discontinuous (or its first derivative with respect to the parameter) change in the geometric phase at the critical point in spin-1/2 XY model [6,7] or Dicke model [8]. This discontinuity also can be observed in open quantum systems induced by dissipation, leading to the so-called dissipative phase transition (DPT) [9–16] and the dynamic optical hysteresis [17–20].

Recently, the observation of optical hysteresis in the driven-dissipative nonlinear Kerr model was reported in experiments [19,20]. It provides a flexible platform for studying DPT [21–23] and stimulates the development of the corresponding theory. In Ref. [24], a metastable theory for the open quantum systems had been established by extending the concept from classical to quantum dynamics, a scope of metastability time was defined, depending on the real part of avoided level crossing in Liouvillian eigenvalue. More recently, it had been demonstrated that the system dynamics

can be described by two Liouvillian eigenvectors whereas the system undergoes DPT and the hysteresis loop is related to the Sarandy-Lidar geometric connection under the observable gauge [25]. The connection describes the geometric property of the Liouville space, and the dynamic optical hysteresis is only one manifestation of it. A closed relation between the hysteresis and the sweeping speed was predicted theoretically and reported experimentally [18–20,25].

Two-level systems (TLS) are the simplest quantum systems that can exist. As a result, the dynamics of a TLS can be solved analytically without any approximation. However, a two-level atom interacting with a quantized mode of an optical cavity provides us with rich physics, such as spontaneous emission and absorption of photons in a cavity. This gives rise to a question whether we can introduce a two-level atom to modulate the hysteresis via its coupling with the cavity in the driven-dissipative nonlinear Kerr model? And if the hysteresis can manifest itself in the dynamics of the atom? In this paper, we will try to answer these questions. We first illustrate the significant relation about the Sarandy-Lidar geometric connection and hysteresis loop and analyze the hysteresis area for the atom and cavity occupation numbers. Then, we show how to achieve our goal and the physical mechanism behind the present scheme is revealed. A feature that the atom-cavity coupling weakens the Kerr nonlinearity in weak coupling regime by mean-field approximation is also predicted. A quantity to describe the relative deviation of the metastable state and target steady state dynamics is also defined. We finally show the dependence of the hysteresis area on the sweeping speed taking only two Liouvillian eigenvectors into account in the composite system.

This paper is structured as follows: We introduce the theoretical framework and present some necessary expressions in Sec. II. In Sec. III, we explore the dynamic optical hysteresis

\*yixx@nenu.edu.cn

in the composite system, reveal the physical mechanism of the modulation, and show how the atom-cavity coupling induced nonlinearity weakens the Kerr nonlinearity in the weak coupling regime. Section IV is devoted to the discussion of dependence of the hysteresis area on the sweeping speed. Finally, we conclude and discuss the results in Sec. V. An Appendix is provided as a supplement to the discussion in the main text.

## II. PHYSICAL MODEL AND THEORETICAL FRAMEWORK

We start by considering a quantum system consisting of a two-level atom resonantly coupled to a cavity with a drive of frequency  $\omega_p$  and Kerr nonlinearity. The Hamiltonian reads ( $\hbar = 1$ )

$$H = -\Delta \left( a^\dagger a + \frac{1}{2} \sigma_z \right) + g(a\sigma_+ + \sigma_- a^\dagger) + \frac{U}{2} a^\dagger a^\dagger a a + F(a + a^\dagger), \quad (1)$$

where  $a^\dagger$  and  $a$ , respectively, are the creation and annihilation operators for the cavity,  $\sigma_+$  and  $\sigma_-$ , respectively, are the raising and lowering operators for the atom with  $\sigma_\pm = \frac{1}{2}(\sigma_x \pm i\sigma_y)$ .  $\Delta = \omega_p - \omega_c$  is the driven-cavity detuning,  $\omega_c$  stands for the cavity frequency,  $g$  denotes the atom-cavity coupling strength,  $U$  is the strength of the Kerr nonlinearity, and  $F$  is the driven amplitude.

Considering the loss of the cavity and the decay of the two-level atom, we write the master equation in Lindblad form to describe the dynamics of density operator  $\rho(t)$ ,

$$\begin{aligned} \frac{d\rho(t)}{dt} = & -i[H, \rho] \\ & + \sum_{m=1}^2 \frac{\kappa_m}{2} n_{th} (2X_m^\dagger \rho X_m - X_m X_m^\dagger \rho - \rho X_m X_m^\dagger) \\ & + \sum_{m=1}^2 \frac{\kappa_m}{2} (1 + n_{th}) (2X_m \rho X_m^\dagger - X_m^\dagger X_m \rho - \rho X_m^\dagger X_m), \end{aligned} \quad (2)$$

where  $H$  is the Hamiltonian of the system.  $n_{th}$  is the photon numbers of the environment.  $\kappa_1$  denotes the decay rate of the cavity, whereas  $\kappa_2$  is the atomic decay rate.  $X_1 = a$  and  $X_2 = \sigma_-$ . The Hilbert space of the system is  $\mathcal{H} \otimes \mathcal{H}$ , which is a tensor product of the cavity and the atom.  $\langle A \rangle := \text{Tr}(A\rho)$  where  $\text{Tr}$  denotes the trace over the system.

Since the master equation (2) is linear in  $\rho(t)$ , we can rewrite it as

$$\frac{d|\rho(t)\rangle}{dt} = \mathcal{L}|\rho(t)\rangle, \quad (3)$$

where  $\mathcal{L}$  is the Liouvillian superoperator and  $|\rho(t)\rangle$  is the vectorized representation for  $\rho(t)$ , called a Dirac-like ket. One can find the unique and initial state-independent steady state  $|\rho_{ss}\rangle$  by solving  $\mathcal{L}|\rho_{ss}\rangle = 0$ . The other eigenvectors of  $\mathcal{L}$  are denoted by  $|\rho^q\rangle$ , and the corresponding nonzero eigenvalues are denoted as

$$\lambda_q = \gamma_q + i\omega_q, \quad (4)$$

where  $q = 1, 2, \dots$  and the eigenvalues of the superoperator are arranged in the decreasing order of  $\gamma_q$ . It has been shown that  $\gamma_q < 0$  ensures the existence of a steady state [26,27], whereas  $\omega_q$  can be treated as the oscillation frequencies. The biorthogonality relation reads

$$(\rho^p | \rho^q) = \delta_{pq}. \quad (5)$$

For a time-independent Liouvillian superoperator  $\mathcal{L}$ , we can expand the vectorized density matrix in terms of the eigenvectors as [27]

$$|\rho(t)\rangle = |\rho^0\rangle + \sum_{q \neq 0} |\rho^q\rangle e^{\lambda_q t} (\rho^q | \rho(t=0)\rangle), \quad (6)$$

where  $|\rho(t=0)\rangle$  denotes the initial state and  $|\rho^0\rangle = |\rho_{ss}\rangle$ . The sum includes all the right eigenvectors of  $\mathcal{L}$ . As shown in the earlier study, for a system undergoing DPT, the sum in Eq. (6) can be approximated to include only the two lowest terms, ignoring the minor impact from the other Liouvillian eigenvectors [25],

$$|\rho(\tau)\rangle = |\rho^0\rangle + |\rho^1\rangle e^{\lambda_1 \tau} (\rho^1 | \rho(t=0)\rangle) + O_{[\lambda_{q>1}]}, \quad (7)$$

this approximation is valid in the region nearby the critical point within a specific timescale  $\tau$  satisfying  $1/|\gamma_2| \ll \tau \ll 1/|\gamma_1|$  [24].

For a time-dependent system, Liouvillian superoperator  $\mathcal{L}$  might depend on time via parameters  $R = (R^1, R^2, \dots)$ ,  $R = R(t)$ . The Sarandy-Lidar geometric connection [28] in this case reads

$$A_{R^n}^{pq} = (\rho_{R^n}^p | \nabla | \rho_{R^n}^q), \quad n = 1, 2, \dots, \quad (8)$$

which describes the geometric property of the Liouville space, where  $R^n$  may be driven amplitude  $F$  [18] or driven-cavity detuning  $\Delta$  [20,25]. Similarly, we consider only two eigenvectors as the earlier study did in the time-independent system whereas the system undergoes DPT [25],

$$|\rho(\tau)\rangle \approx |\rho_{R^n}^0\rangle + \chi_{R^n}^1 |\rho_{R^n}^1\rangle. \quad (9)$$

With this consideration, a concise expression takes

$$A_{R^n}^{10} \equiv (\rho_{R^n}^1 | \nabla | \rho_{R^n}^0) = \gamma_{1,R^n} \alpha_{R^n}^{(1)}, \quad (10)$$

$\alpha_{R^n}^{(1)}$  is the first order expansion coefficient of  $\chi_{R^n}^1$  (for details, see the Appendix). Recall that  $\gamma_{1,R^n}$  is always negative, the sign of  $A_{R^n}^{10}$  is opposite to  $\alpha_{R^n}^{(1)}$ . In this sense, the dynamic optical hysteresis is closely related to the geometric property of the Liouville space.

## III. HYSTERESIS IN THE ATOM-CAVITY SYSTEM

### A. The effect of atom-cavity coupling on the hysteresis area

In this section, we work with a time-periodic change parameter  $\Delta$ , which is swept in an ascending order from  $\Delta_{\min}$  to  $\Delta_{\min} + N \delta\Delta$  and another descending order from  $\Delta_{\min} + N \delta\Delta$  to  $\Delta_{\min}$ , where  $N$  is the number of total steps of sweeping. The study on dynamic sweeping can be dated back to the 1990s past century in the research of optical bistability [29]. Recently, it has been applied to study the hysteresis loop in driven-dissipative systems [18–20,25]. To study the hysteresis behavior, we first solve the master equation at  $\Delta = \Delta_{\min}$  to find the steady state solution and take the solution as the initial

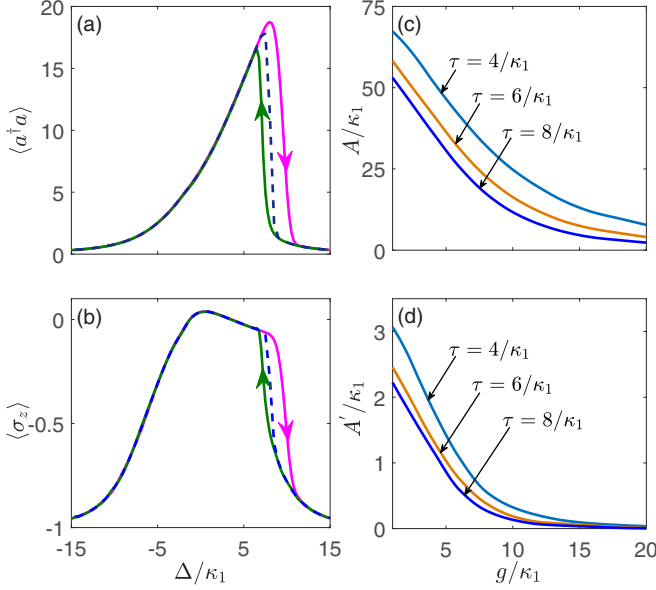


FIG. 1. (a) The cavity occupation numbers  $\langle a^\dagger a \rangle$  and (b)  $\langle \sigma_z \rangle$  as a function of the sweeping parameter  $\Delta$  (in units of  $\kappa_1$ ). In (a) and (b), solid lines stand for the hysteresis loop, whereas the dashed line denotes the steady state solution. The arrows indicate the sweeping direction. (c) and (d) are plotted for the hysteresis area  $A$  and  $A'$  corresponding to the cavity occupation numbers  $\langle a^\dagger a \rangle$  and  $\langle \sigma_z \rangle$ , respectively, as a function of atom-cavity coupling strength  $g$  (in units of  $\kappa_1$ ) for different metastable residence times  $\tau$ . The other system parameters chosen are  $F = 8$ ,  $U = 0.5$ ,  $\kappa_2 = 0.5$  in units of  $\kappa_1$  and  $N = 121$ .

state, then sweep  $\Delta$  in both ascending and descending orders. The sweeping is conducted at a constant speed characterized by  $\delta\Delta$  and a metastable residence time  $\tau$  [20,25]. The results are shown by the solid lines in Figs. 1(a) and 1(b) where we plot both the dynamic hysteresis and the steady state behavior of cavity occupation numbers  $\langle a^\dagger a \rangle$  and the atom  $\langle \sigma_z \rangle$ . Clearly, the results of the steady state is in between the hysteresis loop. It is worth pointing out that the forward (backward) sweeping curves are always on the top (at the bottom) of the steady state solutions, this depends on the sign of  $A_{\Delta}^{10}$  keeping unchanged in the forward (backward) sweeping (as shown in the Appendix Fig. 6).

Next, in order to study the properties of dynamic optical hysteresis quantitatively, we define a hysteresis area enclosed by the hysteresis loop [18–20,25],

$$A = \int_{\Delta_{\min}}^{\Delta_{\max}} |n_{\uparrow} - n_{\downarrow}| d\Delta, \quad (11)$$

where  $\uparrow$  and  $\downarrow$  denote different sweeping directions. The results are shown in Figs. 1(c) and 1(d) where the hysteresis area is plotted as a function of the atom-cavity coupling  $g$  for different  $\tau$ 's corresponding to  $\langle a^\dagger a \rangle$  and  $\langle \sigma_z \rangle$ , respectively. The hysteresis area decreases with the increasing of  $g$  and approaches to zero when the coupling is strong enough. Obviously, we could modulate the dynamic hysteresis feature through changing the atom-cavity coupling.

In order to get more information when we introduce the two-level atom into the system, we define a witness which

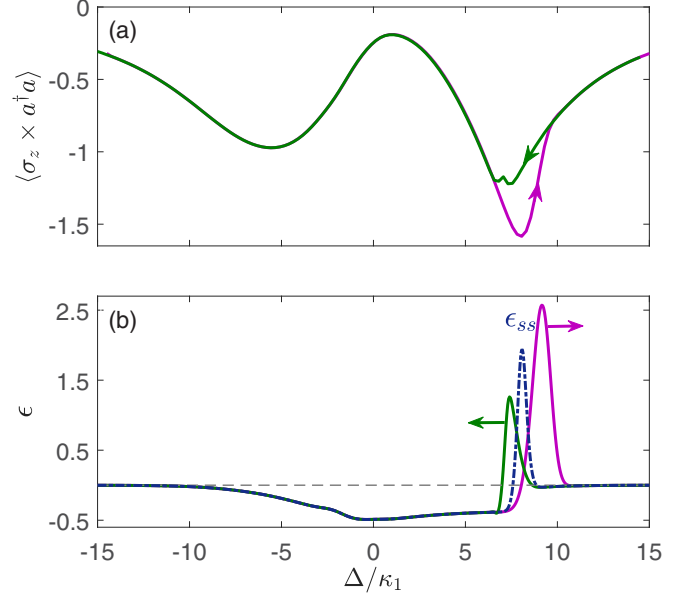


FIG. 2. (a) The hysteresis loop for the joint operator  $\langle \sigma_z \times a^\dagger a \rangle$  and (b) the witness  $\epsilon$  averaged over the steady (dashed-dot line) and metastable (solid lines) state with  $\tau = 8/\kappa_1$  as a function of  $\Delta$  (in units of  $\kappa_1$ ). The gray dashed line corresponds to  $\epsilon = 0$ . The arrows indicate the sweeping direction. The other system parameters are the same as in Fig. 1.

characterizes the validity of mean-field approximation in this system by

$$\epsilon = \langle \sigma_z a^\dagger a \rangle - \langle \sigma_z \rangle \langle a^\dagger a \rangle. \quad (12)$$

We first calculate  $\langle \sigma_z a^\dagger a \rangle$  whereas sweeping  $\Delta$  through the critical region. The numerical results are shown in Fig. 2(a) where a hysteresis can be found. Next we plot  $\epsilon$  as a function of  $\Delta$  averaged over both the metastable and steady state. As expected, the peak of  $\epsilon_{ss}$  for the steady state is between that of forward and backward sweepings. In the next section, we will show that all the hysteresis features in this section can be interpreted by the discontinuity of the first nonzero Liouvillian eigenvalue, and the decreasing of the hysteresis area is closely related to the effect of atom-cavity coupling on the discontinuity of that eigenvalue.

### B. The fundamental mechanisms of the modulation

In order to reveal the physics behind the modulation, we calculate and discuss the first ( $q = 1$ ) nonzero eigenvalue of  $\mathcal{L}$  in the zero-temperature limit in this section. As shown in Fig. 3, the real part of the first nonzero eigenvalue  $\lambda_1$  undergoes a sharp change in a critical point  $\Delta$  depending on the atom-cavity coupling, which leads to a long-time metastable dynamics [24]. The critical point moves and disappears gradually with the increasing in  $g$ . This is consistent with the decreasing of hysteresis area  $A$  with the increasing in atom-cavity coupling strength. On the contrary, the hysteresis behavior would disappear in a general system without DPT. Here, we point out the imaginary part of  $\lambda_1$  is zero and not degenerate when the system parameters are chosen nearby

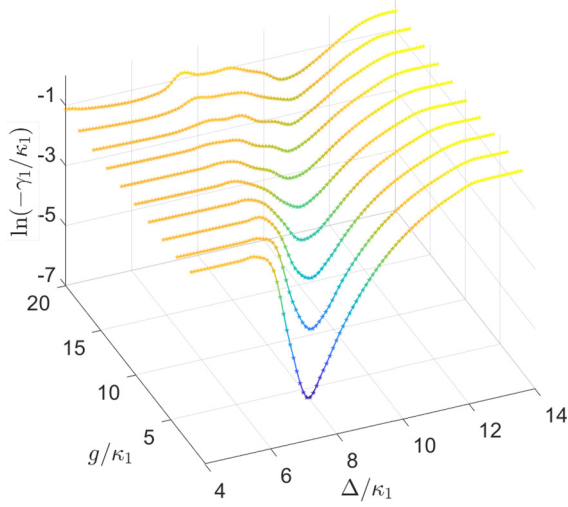


FIG. 3. The first nonzero eigenvalue  $\ln(-\gamma_1/\kappa_1)$  of the Liouvillian superoperator as a function of driven-cavity detuning  $\Delta$  (in units of  $\kappa_1$ ) and atom-cavity coupling constant  $g$  (in units of  $\kappa_1$ ), the discontinuity of the first nonzero Liouvillian eigenvalue vanishes in the function of  $\Delta$  when the coupling is strong enough. Other system parameters are the same as in Fig. 1.

the critical point, which indicates that the dynamics is not of oscillation and  $\rho^1$  is Hermitian [16].

As a comparison, we also analyze the real part of  $\lambda_2$ , there is a similar behavior to  $\lambda_1$ . The difference is the critical region of  $\lambda_2$  is substantially narrowed, and the dip of the Liouvillian eigenvalue becomes shallow. Therefore, considering the other eigenvectors ( $q > 2$ ) would contribute less to the dynamics if we focus on a specific time  $\tau$  in the range of  $1/-\gamma_2 \ll \tau \ll 1/-\gamma_1$  [24]. In the next section, we would mainly focus on the contribution of  $\rho^0$  and  $\rho^1$  to the dynamics.

For this purpose, we first ignore the jump term  $X_m \rho X_m^\dagger$  in the master equation and rewrite it as

$$\frac{d\rho(t)}{dt} = -i[H, \rho] - \sum_{m=1}^2 \frac{\kappa_m}{2} \{X_m^\dagger X_m, \rho\} = \tilde{\mathcal{L}}\rho, \quad (13)$$

where  $\tilde{\mathcal{L}}$  is the effective non-Hermitian Liouvillian superoperator. We perform the same calculation for  $\tilde{\mathcal{L}}$  and show  $\ln(-\tilde{\gamma}_1)$  as a function of  $\Delta$  in Fig. 4. There is no discontinuity, and we claim that the discontinuity of first nonzero Liouvillian eigenvalue attributes to the effect of  $X_m \rho X_m^\dagger$  in our system.

### C. Weakening of the nonlinearity caused by atom-cavity couplings

We have shown that the decrease in hysteresis area  $A$  with the increase in atom-cavity coupling  $g$  is related to the effect of the atom-cavity coupling on the discontinuity of the first nonzero Liouvillian eigenvalue. One may wonder what is the physics behind this observation? As shown in Refs. [10,30], the coupling between the field and the atom can cause Kerr nonlinearity. In the following, we will demonstrate that the nonlinearity induced by atom-cavity coupling weakens the Kerr nonlinearity in the weak coupling regime, leading to a change in the critical point and, consequently, the decrease in the hysteresis area. Now we go to the details.

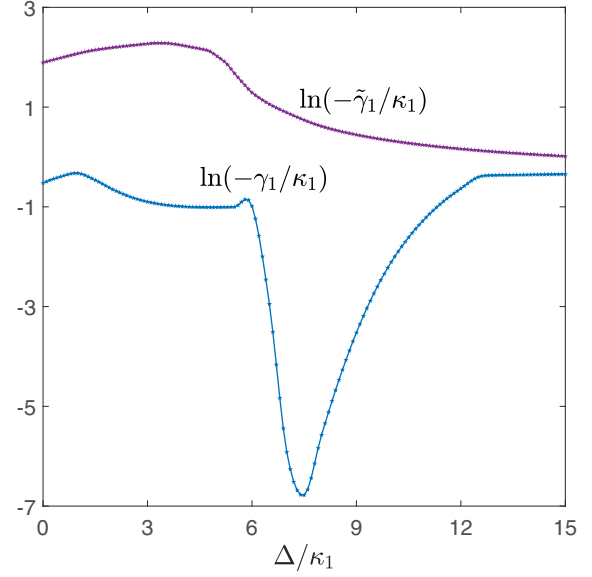


FIG. 4.  $\ln(-\tilde{\gamma}_1/\kappa_1)$  and  $\ln(-\gamma_1/\kappa_1)$  as a function of driven-cavity detuning  $\Delta$  (in units of  $\kappa_1$ ) with  $g/\kappa_1 = 1$ . The other system parameters are the same as in Fig. 1.

By the mean-field approximation, we obtain the following equations from the Hamiltonian in Eq. (1) [31,32],

$$\dot{\alpha} = (i\Delta - iU|\alpha|^2 - \kappa)\alpha - ig\beta - iF, \quad (14)$$

$$\dot{\beta} = -(\gamma_\perp - i\Delta)\beta + ig\alpha\xi, \quad (15)$$

$$\dot{\xi} = 2ig(\alpha^*\beta - \alpha\beta^*) - \gamma_\parallel(\xi + 1), \quad (16)$$

where  $\alpha = \langle a \rangle$ ,  $\beta = \langle \sigma_- \rangle$ , and  $\xi = \langle \sigma_z \rangle$ .  $\gamma_\perp$  and  $\gamma_\parallel$  denote the transverse and longitudinal relaxation rates of the atom, respectively [32]. Simple algebra yields the steady state solutions of  $\alpha$  and  $\xi$ ,

$$\alpha = \frac{iF}{i\Delta - \kappa - iU|\alpha|^2 + \frac{g^2\xi}{\gamma_\perp - i\Delta}}, \quad (17)$$

$$\xi = \frac{-1}{1 + \frac{4g^2|\alpha|^2}{\gamma_\perp\gamma_\parallel(1 + \frac{\Delta^2}{\gamma_\perp^2})}}. \quad (18)$$

Here, we consider the linear relation  $\gamma_\perp = m\gamma_\parallel$  where  $m$  is a constant. In this case, the results reduce to

$$\alpha = \frac{iF}{i\Delta - \kappa - iU|\alpha|^2 - \frac{g^2(\gamma_\perp + i\Delta)}{\gamma_\perp^2 + \Delta^2 + 4mg^2|\alpha|^2}}. \quad (19)$$

In the weak coupling regime defined by [10]

$$4mg^2|\alpha|^2 \ll \Delta^2, \quad (20)$$

and consider  $\gamma_\perp$  is very small compared to the detuning  $\Delta$  [32], we obtain

$$\alpha = \frac{iF}{-i(U - \frac{4mg^4}{\Delta^3})|\alpha|^2 + f(\gamma_\perp) - i\frac{g^2}{\Delta} + i\Delta - \kappa}, \quad (21)$$

where

$$f(\gamma_\perp) = \frac{g^2\gamma_\perp^3 + ig^2\Delta\gamma_\perp^2 - g^2\Delta^2\gamma_\perp + 4mg^4\gamma_\perp|\alpha|^2}{\Delta^4}$$

can be treated as the effect of atomic decay. The term with  $-\frac{4mg^4}{\Delta^3}$  weakens the Kerr nonlinearity. We should point out it leads to the same conclusion whereas the Kerr nonlinearity strength  $U < 0$  for the corresponding critical point also appears at  $\Delta < 0$ .

#### IV. THE HYSTERESIS AREA

In the previous section, we have shown the hysteresis with a constant sweeping speed. It is the nonadiabatic response of the driven-dissipative system at a timescale that the sweeping is much shorter than the typical timescale of the system [18]. At such a metastable timescale, the dynamics can be described by two Liouvillian eigenvectors [25]. It is natural to ask: Whether we can obtain an expression for the hysteresis area within the above approximation? And if the linear dependence of the hysteresis area on the sweeping speed remains whereas a two-level atom is introduced in the limit of slow sweeping? We will answer those questions in the following. We would like to note that the approach introduced here is quite different from Ref. [18] in which the treatment was based on the width of the nonadiabatic region nearby the critical point, whereas in our case we analyze the dynamics of the system with sweepings.

First, we discuss the relation between the hysteresis and the adiabaticity of the evolution. With a constant metastable residence time, increasing  $N$  equals to decreasing  $\delta\Delta$ . To characterize the adiabaticity, we define  $\zeta$  as the difference of the mean photon numbers between the metastable and the steady state,

$$\zeta = \frac{n_{\Delta_k}^\tau}{n_{\Delta_{k+1}}^0} - 1, \quad (22)$$

where  $n_{\Delta_k}^\tau = \text{Tr}(a^\dagger a \rho_{\Delta_k}^\tau)$  and  $n_{\Delta_{k+1}}^0 = \text{Tr}(a^\dagger a \rho_{\Delta_{k+1}}^0)$ . We show  $\zeta$  as a function of  $\Delta$  for different  $N$ 's in Fig. 5(a). Obviously,  $\zeta = 0$  corresponds that the system undergoes adiabatic evolution. With the increasing in  $N$ , the nonzero region of  $\zeta$  approaches zero gradually nearby the critical point. Therefore, the state of the system would exactly follow the instantaneous steady state of open quantum systems if the parameter changes infinitely slowly [33,34].

With this knowledge, we now discuss the hysteresis area. When the driven-cavity detuning changes, the system state evolves from the initial metastable state towards the target steady state leading by the Liouvillian superoperator with the changed detuning. In Fig. 5(b), we show the hysteresis area  $A$  as a function of  $v^{-1}$ , where  $v$  is defined as [25]

$$v = \frac{\Delta_{\max} - \Delta_{\min}}{N\tau} = \frac{\delta\Delta}{\tau}. \quad (23)$$

Taking only two Liouvillian eigenvectors into account and performing the Taylor expansion on  $e^{\lambda_1\tau}$ . Ignoring the high order ( $n \geq 2$ ) of  $\lambda_1\tau$ , we obtain

$$\begin{aligned} |\rho_{\Delta_{k+1}}^\tau\rangle &= |\rho_{\Delta_{k+1}}^0\rangle + C_{\Delta_{k+1}}^1 e^{\lambda_1\tau} |\rho_{\Delta_{k+1}}^1\rangle \\ &= |\rho_{\Delta_{k+1}}^0\rangle + C_{\Delta_{k+1}}^1 (1 + \lambda_1\tau) |\rho_{\Delta_{k+1}}^1\rangle, \end{aligned} \quad (24)$$

where “+” denotes that  $\Delta$  is in ascending order from  $\Delta_{\min}$ .  $C_{\Delta_{k+1}}^1 = \langle \rho_{\Delta_{k+1}}^1 | \rho_{\Delta_k}^\tau \rangle$  are the expansion coefficients. As for the backward sweeping from  $\Delta_{\max}$ , which is labeled by

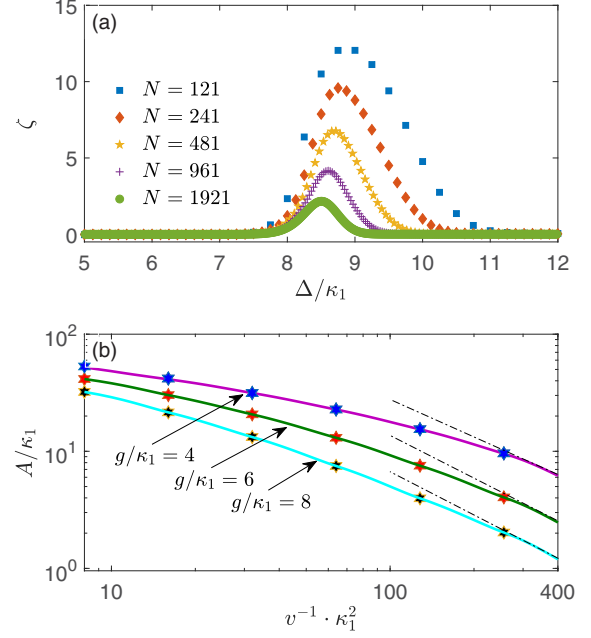


FIG. 5. (a)  $\zeta$  as a function of driven-cavity detuning  $\Delta$  (in units of  $\kappa_1$ ) for different  $N$ 's at the same metastable residence time  $\tau = 4/\kappa_1$ . (b) The hysteresis area  $A$  as a function of sweeping speed  $v^{-1}$  (in units of  $\kappa_1^{-2}$ ) with different atom-cavity coupling constant  $g$ . The calculation is performed with all the Liouvillian eigenvectors. Black dashed lines are the asymptotic lines, and the hexagrams are the numerical results of Eq. (26). The other parameters are the same as in Fig. 1.

$|\rho_{\Delta_{N-k}}^\tau\rangle$  and  $C_{\Delta_{N-k}}^1 = \langle \rho_{\Delta_{N-k}}^1 | \rho_{\Delta_{N-(k-1)}}^\tau \rangle$  with  $\Delta_k = \Delta_{N-k}$ . Similarly, “-” denotes  $\Delta$  is in descending order from  $\Delta_{\max}$ . Substituting Eq. (23) into Eq. (24), we obtain the expression of  $|\rho_{\Delta_{k+1}}^\tau\rangle$  to  $v^{-1}$  as

$$|\rho_{\Delta_{k+1}}^\tau\rangle = |\rho_{\Delta_{k+1}}^0\rangle + C_{\Delta_{k+1}}^1 (1 + \lambda_1\delta\Delta v^{-1}) |\rho_{\Delta_{k+1}}^1\rangle, \quad (25)$$

Substituting Eq. (25) into Eq. (11) and choosing the constraint  $\text{Tr}(\rho_{\Delta_k}^1 a^\dagger a) = 1$  [25], the hysteresis area  $A$  reads (a substitution for  $k+1$  to  $k$ ),

$$A = \int_{\Delta_{\min}}^{\Delta_{\max}} (C_{\Delta_k}^1 - C_{\Delta_{N-k}}^1) (1 + \lambda_1\delta\Delta v^{-1}) d\Delta. \quad (26)$$

We note that  $v$  is the denominator in Eq. (26), the hysteresis area seems diverging to infinity in the limit of  $v \rightarrow 0$ . This is not true when we take  $C_{\Delta_k}^1 - C_{\Delta_{N-k}}^1$  into consideration. In fact,  $C_{\Delta_k}^1 - C_{\Delta_{N-k}}^1$  approaches to zero in the slow sweeping limit. This is shown in Fig. 5(b) (hexagrams) which are in good agreement with the numerical results involving all eigenvectors of the Liouvillian. Besides, we find that  $A$  decreases with the increasing in  $v^{-1}$ , and it obeys a linear power law decay with the sweeping, see Fig. 5(b). There is only a small hysteresis area left, and the slope of the decreasing is very small. In this regime, the slope is almost independent of  $v$ , which could be regarded as a constant corresponding to the asymptotically linear region.

## V. CONCLUSION

In this paper, introducing a two-level atom into a nonlinear dissipative cavity, we have studied the dynamics of the atom and found a hysteresis feature in the dynamics. The hysteresis could be modulated by the atom-cavity coupling strength and the dependence of the hysteresis area on the coupling was analyzed. The physics behind the modulation can be understood as the change in the critical point due to the atom-cavity coupling. We also examined the role played by the jump terms in the master equation and found that the jump term might lead to the discontinuity of the first nonzero Liouvillian eigenvalue, and the nonlinearity induced by atom-cavity coupling weakens the Kerr nonlinearity in weak coupling regime. A quantity  $\zeta$  was introduced to measure the relation between hysteresis and adiabaticity of the evolution. Its dependence on the sweeping is given. Finally, we have illustrated the dependence of the hysteresis areas on the sweeping, taking only two Liouvillian eigenvalues into account.

## ACKNOWLEDGMENTS

This work was supported by National Natural Science Foundation of China (NSFC) under Grants No. 11775048 and No. 12047566.

## APPENDIX: THE DERIVATION OF SARANDY-LIDAR GEOMETRIC CONNECTION

In this Appendix, the Sarandy-Lidar geometric connection is derived based on Ref. [25], which is helpful to understand the geometric property of the Liouville space intuitively.

Here, we emphasize that the Liouvillian superoperator is time dependent caused by  $R^n(t)$  in the parameter space.  $|\rho(t)\rangle\rangle$  can be expanded in the right instantaneous eigenvectors of  $\mathcal{L}^{R^n}$ ,

$$|\rho(t)\rangle\rangle = \sum_{q=0} \chi_{R^n}^q |\rho_{R^n}^q\rangle\rangle, \quad (\text{A1})$$

where  $\chi_{R^n}^q$ 's are the time-dependent expansion coefficients and usually complex (except  $\chi_{R^n}^1$  nearby the critical point). Then, plug Eq. (A1) into master equation (3), project on  $\langle\rho^p|$  and use the biorthogonality relation (5), leading to

$$\dot{\chi}_{R^n}^p + \sum_{q=0} \chi_{R^n}^q \langle\rho_{R^n}^p| \frac{d}{dt} |\rho_{R^n}^q\rangle\rangle = \lambda_{p,R^n} \chi_{R^n}^p, \quad (\text{A2})$$

Finally, we plug the differential expression of Eq. (23),  $v = dR^n/dt$ , and the result can be written as

$$\frac{d}{dR^n} \chi_{R^n}^p + \sum_{q=0}^q A_{R^n}^{pq} \chi_{R^n}^q = \frac{1}{v} \lambda_{p,R^n} \chi_{R^n}^p, \quad (\text{A3})$$

where

$$A_{R^n}^{pq} = \langle\rho_{R^n}^p| \frac{d}{dR^n} |\rho_{R^n}^q\rangle\rangle \quad (\text{A4})$$

is the Sarandy-Lidar geometric connection.

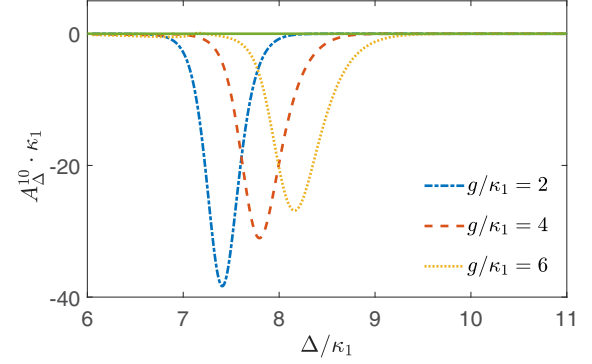


FIG. 6. Sarandy-Lidar geometric connection  $A_{\Delta}^{10}$  as a function of driven-cavity detuning  $\Delta$  (in units of  $\kappa_1$ ) for different coupling strengths. The solid line corresponds to  $A_{\Delta}^{10}\kappa_1 = 0$ . The other system parameters are the same as in Fig. 1.

Next, analogy to the approximation in the time-independent system, the sum in Eq. (A1) can be truncated at  $q = 2$ , the contribution of other eigenvectors to the dynamics is negligible,

$$|\rho(t)\rangle\rangle \approx \chi_{R^n}^0 |\rho_{R^n}^0\rangle\rangle + \chi_{R^n}^1 |\rho_{R^n}^1\rangle\rangle, \quad (\text{A5})$$

where  $|\rho_{R^n}^0\rangle\rangle$  is the steady state and  $\chi_{R^n}^0 = 1$  always sets up. We can calculate the cavity occupation numbers by  $n(t) = \text{Tr}[a^\dagger a \rho(t)]$ , leading to

$$n(t) = n_{R^n}^{\text{st}} + \chi_{R^n}^1, \quad (\text{A6})$$

with the observable gauge  $\text{Tr}(a^\dagger a \rho_{R^n}^1) = 1$ . Then, at small  $v$ , we expand  $\chi_{R^n}^1$  into

$$\chi_{R^n}^1 = \sum_{s=1}^{\infty} \alpha_{R^n}^{(s)} v^s, \quad (\text{A7})$$

where  $\alpha_{R^n}^{(s)}$  is the  $s$ th order expansion coefficient. Inserting it into Eq. (A6) and ignoring the high order of  $v$ ,

$$n_{R^n} \approx n_{R^n}^{\text{st}} + \alpha_{R^n}^{(1)} v. \quad (\text{A8})$$

In addition, due to the truncated in Eq. (A5), we can extract an ordinary differential equation from Eq. (A3) about  $\chi_{R^n}^1$ ,

$$\frac{d}{dR^n} \chi_{R^n}^1 + A_{R^n}^{10} + \left( A_{R^n}^{11} - \frac{\lambda_1}{v} \right) \chi_{R^n}^1 = 0. \quad (\text{A9})$$

Similarly, inserting Eq. (A7) into Eq. (A9) and substituting  $\lambda_1$  with  $\gamma_1$ , we obtain

$$A_{R^n}^{10} = \gamma_{1,R^n} \alpha_{R^n}^{(1)}. \quad (\text{A10})$$

Now, it is clear that the hysteresis loop is relevant to the Sarandy-Lidar geometric connection  $A_{R^n}^{10}$  from Eqs. (A8) and (A10), we can obtain a significant property that the Sarandy-Lidar geometric connection is positive or negative depending on  $\alpha_{R^n}^{(1)}$  which is associated with the direction of dynamic sweeping. As shown in Fig. 6, Sarandy-Lidar geometric connection  $A_{\Delta}^{10}$  is always nonpositive in forward sweeping.

- [1] L. D. Landau and E. M. Lifshitz, *Statistical Physics* (Pergamon, Oxford, 1969).
- [2] S. Sachdev, *Quantum Phase Transitions* (Cambridge University Press, Cambridge, UK, 2011).
- [3] Y. H. Kim, N. Kaur, B. M. Atkins, N. S. Dalal, and Y. Takano, Fluctuation-Induced Heat Release from Temperature-Quenched Nuclear Spins near a Quantum Critical Point, *Phys. Rev. Lett.* **103**, 247201 (2009).
- [4] X. Li, J.-R. Wang, and G.-Z. Liu, Phase transition with trivial quantum criticality in an anisotropic Weyl semimetal, *Phys. Rev. B* **97**, 184508 (2018).
- [5] T. Yamamoto and T. Kato, Quantum critical phenomena in heat transport via a two-state system, *Phys. Rev. B* **98**, 245412 (2018).
- [6] A. C. M. Carollo and J. K. Pachos, Geometric Phases and Criticality in Spin-Chain Systems, *Phys. Rev. Lett.* **95**, 157203 (2005).
- [7] S.-L. Zhu, Scaling of Geometric Phases Close to the Quantum Phase Transition in the XY Spin Chain, *Phys. Rev. Lett.* **96**, 077206 (2006).
- [8] G. Chen, J.-Q. Li, and J.-Q. Liang, Critical property of the geometric phase in the Dicke model, *Phys. Rev. A* **74**, 054101 (2006).
- [9] E. M. Kessler, G. Giedke, A. Imamoglu, S. F. Yelin, M. D. Lukin, and J. I. Cirac, Dissipative phase transition in a central spin system, *Phys. Rev. A* **86**, 012116 (2012).
- [10] H. J. Carmichael, Breakdown of Photon Blockade: A Dissipative Quantum Phase Transition in Zero Dimensions, *Phys. Rev. X* **5**, 031028 (2015).
- [11] M.-J. Hwang, P. Rabl, and M. B. Plenio, Dissipative phase transition in the open quantum Rabi model, *Phys. Rev. A* **97**, 013825 (2018).
- [12] F. Vicentini, F. Minganti, R. Rota, G. Orso, and C. Ciuti, Critical slowing down in driven-dissipative Bose-Hubbard lattices, *Phys. Rev. A* **97**, 013853 (2018).
- [13] S. S. Sahoo, S. S. Nayak, S. R. Mishra, and A. K. Mohapatra, Dissipative phase transition in a mirrorless optical parametric oscillator, *Phys. Rev. A* **102**, 053724 (2020).
- [14] J. Gosner, B. Kubala, and J. Ankerhold, Relaxation dynamics and dissipative phase transition in quantum oscillators with period tripling, *Phys. Rev. B* **101**, 054501 (2020).
- [15] W. Casteels, R. Fazio, and C. Ciuti, Critical dynamical properties of a first-order dissipative phase transition, *Phys. Rev. A* **95**, 012128 (2017).
- [16] F. Minganti, A. Biella, N. Bartolo, and C. Ciuti, Spectral theory of Liouvillians for dissipative phase transitions, *Phys. Rev. A* **98**, 042118 (2018).
- [17] N. N. Rosanov, *Spatial Hysteresis and Optical Patterns* (Springer, Berlin, 2002).
- [18] W. Casteels, F. Storme, A. Le Boité, and C. Ciuti, Power laws in the dynamic hysteresis of quantum nonlinear photonic resonators, *Phys. Rev. A* **93**, 033824 (2016).
- [19] S. R. K. Rodriguez, W. Casteels, F. Storme, N. Carlon Zambon, I. Sagnes, L. Le Gratiet, E. Galopin, A. Lemaître, A. Amo, C. Ciuti, and J. Bloch, Probing a Dissipative Phase Transition via Dynamical Optical Hysteresis, *Phys. Rev. Lett.* **118**, 247402 (2017).
- [20] Z. Geng, K. J. H. Peters, A. A. P. Trichet, K. Malmir, R. Kolkowski, J. M. Smith, and S. R. K. Rodriguez, Universal Scaling in the Dynamic Hysteresis, and Non-Markovian Dynamics, of a Tunable Optical Cavity, *Phys. Rev. Lett.* **124**, 153603 (2020).
- [21] T. L. Heugel, M. Biondi, O. Zilberberg, and R. Chitra, Quantum Transducer Using a Parametric Driven-Dissipative Phase Transition, *Phys. Rev. Lett.* **123**, 173601 (2019).
- [22] B. O. Goes and G. T. Landi, Entropy production dynamics in quench protocols of a driven-dissipative critical system, *Phys. Rev. A* **102**, 052202 (2020).
- [23] B. O. Goes, C. E. Fiore, and G. T. Landi, Quantum features of entropy production in driven-dissipative transitions, *Phys. Rev. Research* **2**, 013136 (2020).
- [24] K. Macieszczak, M. Guta, I. Lesanovsky, and J. P. Garrahan, Towards a Theory of Metastability in Open Quantum Dynamics, *Phys. Rev. Lett.* **116**, 240404 (2016).
- [25] D. O. Krimer and M. Pletyukhov, Few-Mode Geometric Description of a Driven-Dissipative Phase Transition in an Open Quantum System, *Phys. Rev. Lett.* **123**, 110604 (2019).
- [26] H. P. Breuer and F. Petruccione, *The Theory of Open Quantum Systems* (Oxford University Press, Oxford, 2007).
- [27] Á. Rivas and S. F. Huelga, *Open Quantum Systems: An Introduction*, Springer Briefs in Physics (Springer, Berlin, 2011).
- [28] M. S. Sarandy and D. A. Lidar, Abelian and non-Abelian geometric phases in adiabatic open quantum systems, *Phys. Rev. A* **73**, 062101 (2006).
- [29] G. Rempe, R. J. Thompson, R. J. Brecha, W. D. Lee, and H. J. Kimble, Optical Bistability and Photon Statistics in Cavity Quantum Electrodynamics, *Phys. Rev. Lett.* **67**, 1727 (1991).
- [30] G. P. Agrawal and H. J. Carmichael, Optical Bistability through Nonlinear Dispersion and Absorption, *Phys. Rev. A* **19**, 2074 (1979).
- [31] M. J. Martin, D. Meiser, J. W. Thomsen, Jun Ye, and M. J. Holland, Extreme nonlinear response of ultranarrow optical transitions in cavity QED for laser stabilization, *Phys. Rev. A* **84**, 063813 (2011).
- [32] D. O. Krimer, M. Zens, and S. Rotter, Critical phenomena and nonlinear dynamics in a spin ensemble strongly coupled to a cavity. I. Semiclassical approach, *Phys. Rev. A* **100**, 013855 (2019).
- [33] L. C. Venuti, T. Albash, D. A. Lidar, and P. Zanardi, Adiabaticity in open quantum systems, *Phys. Rev. A* **93**, 032118 (2016).
- [34] S. L. Wu, X. L. Huang, and X. X. Yi, Fast trajectory tracking of the steady state of open quantum systems, *Phys. Rev. A* **99**, 042115 (2019).